Journal of Materials Chemistry A

PAPER

View Article Online
View Journal | View Issue

Cite this: J. Mater. Chem. A, 2017, 5, 18770

A molecular-level superhydrophobic external surface to improve the stability of metal–organic frameworks†

Yuxiu Sun,[ab] Qi Sun,[b] Hongliang Huang,[c] Briana Aguila,[b] Zheng Niu,[b] Jason A. Perman *[b] and Shengqian Ma *[b]

Received 4th July 2017
Accepted 10th August 2017

DOI: 10.1039/c7ta05800d

rsc.li/materials-a

In this work, we demonstrate a facile molecular-level modification method that imparts superhydrophobic character to Zr-based MOFs, while retaining their high porosity. Alkyl phosphonic acids, such as *n*-octadecylphosphonic acid (OPA), interact with the zirconium oxide clusters situated near and on the surface of the MOF. The octadecyl alkyl chains reduce the surface free energy on the MOF's exterior, yielding a superhydrophobic material with a contact angle greater than 150°. After exposure to aqueous solutions with a high pH and high ionic strength, the OPA-MOFs retain nearly identical surface areas. Notably, the OPA-MOFs are capable of separating organic liquids from water, which could facilitate oil/water separation applications in the event of an oil spill.

Introduction

Metal–organic frameworks (MOFs) are a crystalline class of porous materials, containing metal ions and organic molecules coordinated together in a controlled manner to improve several key features over their traditional porous inorganic and organic counterparts such as zeolites and activated carbons.[1] Apart from their wide structural diversity with adjustable pore sizes, ranging from a few angstroms to several nanometers, and sometimes flexible behaviour, one of their remarkable advantages lies in the possibility of chemical functionalisation, pre- or post-synthesis on the organic ligands or metal ions.[2,3] Earlier studies laid their emphasis on MOFs bearing polar functional groups (NH_2, CO_2H, and SO_3H) and discussed how these groups and their modifications impacted gas adsorption, molecular separations, and chemical catalysis.[4] Yet few have documented a method to modify the MOF's surface to endow them with superhydrophobicity, while retaining access to their porous interior. This requirement arises because many MOFs show poor water stability properties that hinder their open-air applications under humid conditions.[5,6] Even when the water stability is sufficient, these MOFs continue to show lower performance benchmarks under humid conditions or when exposed to acidic/basic conditions. To overcome these hurdles MOFs with (super)hydrophobic properties have been proposed to outperform non-hydrophobic MOFs in terms of their roles in real-world applications.

A limited number of concepts have been reported for imparting hydrophobicity to MOFs.[7–9] Among these strategies, the most common ways include introducing alkyl or fluorinated groups (F, CF_3, and so on)[10–14] or by coating the MOF crystals with a hydrophobic polymer layer.[15–19] These layers interact very weakly with water and do not promote the spreading of water droplets on their surface.[20] However, these hydrophobic MOFs are usually realized through the introduction of hydrophobic molecular linkers, requiring new and sometimes tedious procedures, which reduces the material's surface area or results in materials that fail to remain intact under environmental conditions where high or low pH and high ionic strength solutions are found. Therefore, a facile approach has been developed to realize hydrophobic porous MOFs that retain much of their original properties and find broader use.

Alkylphosphonic acids with a long alkyl chain end $[CH_3(CH_2)_nP(O)(OH)_2]$ ($n > 6$) can be coordinated to metals (Ti, Zr, Zn, Al, *etc.*) with strong M–O–P bonds. This can enhance the material's physical properties and improve its hydrophobicity or its resistance to corrosion.[21,22] It is also evident that octadecylphosphonic acid (OPA) can be chemisorbed from solution to the $BaTiO_3$ surface through bidentate bonding of the alkylphosphonic acid moieties with the oxide.[23] These reports inspired us to develop a facile strategy of imparting alkylphosphonic acid molecules on the outer surface of MOFs to obtain superhydrophobicity without altering the intact structure and inner channel environment of the MOFs. Intentionally, we selected Zr-based MOFs (such as UiO-66, UiO-66-SO_3H, and PCN-222), believed to be promising in future applications due to their structural stability, to serve as the prototype host materials; and

[a]Tianjin International Joint Research Centre of Surface Technology for Energy Storage Materials, College of Physics and Materials Science, Tianjin Normal University, Tianjin 300387, China

[b]Department of Chemistry, University of South Florida, 4202 E. Fowler Avenue, Tampa, Florida 33620, USA. E-mail: sqma@usf.edu; perman@usf.edu

[c]State Key Laboratory of Organic-Inorganic Composites, Beijing University of Chemical Technology, Beijing 100029, China

† Electronic supplementary information (ESI) available. See DOI: 10.1039/c7ta05800d

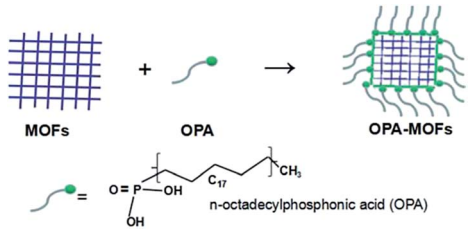

Scheme 1 Molecular-level external modification of superhydrophobic MOFs utilizing OPA.

OPA as the classic alkylphosphonic acid, which would provide a low energy surface and a high level of hydrophobicity (Scheme 1). The long alkyl chains positioned on the MOF's surface would not block the inherent porosity of the frameworks, but generate high water resistance and keep them stable under various aqueous conditions. Our design is a facile and molecular-level approach for realizing superhydrophobic MOF materials that will show improved capability for some practical applications.

Experimental

Materials

All chemical reagents were purchased and used without further purification: zirconium(IV) chloride ($ZrCl_4$, Aldrich, 98%), terephthalic acid (BDC, TCI, >99%), monosodium 2-sulfoterephthalate (2-$NaSO_3$-H_2BDC, TCI, >98%), *n*-octadecylphosphonic acid (OPA, Alfa Aesar, 97%), *N*,*N*-dimethylformamide (DMF, Fisher Scientific), *N*,*N*-diethylformamide (DEF, TCI), methyl 4-formylbenzoate (Sigma-Aldrich), pyrrole (Sigma-Aldrich), methanol, acetone, and ethanol (Fisher Scientific), NaCl and Na_2SO_4 (Aldrich), 1-naphthalenesulfonic acid (NA, Aldrich, 50%), and toluene and benzene (Sigma-Aldrich).

Instrumentation

Powder X-ray diffraction (PXRD) measurements were recorded from a BRUKER D8 ADVANCE X-ray diffractometer equipped with graphite mono-chromatized Cu Kα radiation ($\lambda = 1.54056$ Å) at 40 kV and 40 mA. The morphologies of the MOFs were characterized using a Hitachi S-4700 scanning electron microscope (SEM) with an accelerating voltage of 20.0 kV. Elemental line-scanning and mapping were conducted with EDX microanalysis (EDX/JEM-2100F, 200 kV). Water contact angle measurements were carried out using a KSV CAM 100 optical contact angle meter under ambient conditions. N_2 adsorption–desorption isotherms were measured using a Micromeritics ASAP 2020 system at 77 K. The specific surface area is acquired using the Brunauer–Emmett–Teller (BET) method. The carbon dioxide adsorption–desorption isotherms were measured using an adsorption instrument (Micromeritics ASAP 2020). Fourier transform infrared (FT-IR) measurements were performed on a PerkinElmer FT-IR C94349 spectrometer. The grafting content of OPA on MOFs was determined using an inductively coupled plasma-optical emission spectrometer (ICP-OES, Thermo iCAP-6300). UV-Vis data were collected using a Jasco V-670 UV-vis-NIR spectrophotometer.

Synthesis of UiO-66

UiO-66 was synthesized according to the previous report with minor modifications.[24] Typically, $ZrCl_4$ (80 mg, 0.343 mmol) and BDC (57 mg, 0.343 mmol) were dissolved in DMF (20 mL) at room temperature under vigorous stirring. The mixture was then sealed in a Teflon reactor (20 mL), heated to 120 °C and maintained for 48 h. After cooling down to room temperature, the precipitate was recovered by centrifugation and washed with fresh DMF three consecutive times. Then the solids were immersed in methanol overnight. Finally, the resulting white powder was dried at 120 °C for 24 h.

Synthesis of UiO-66-SO_3H

The MOF was synthesized according to the previous report.[25] For UiO-66-SO_3H $[Zr_6O_4(OH)_4(HSO_3BDC)_{6x}(BDC)_{6-6x}$, $(x = 0.18)]$, 53 mg of $ZrCl_4$ was added to 61 mg of 2-$NaSO_3$-H_2BDC in a 20 mL glass vial. 9 mL of DMF and 1 mL of acetic acid were then added. The vial was sealed with a Teflon cap and heated for 40 h at 120 °C. The product was then suction filtered and washed with DMF and diethyl ether, followed by air-drying.

Synthesis of PCN-222

The organic ligand (tetrakis(4-carboxyphenyl)-porphyrin, H_2TCPP) and PCN-222 were synthesized based on the previous report.[26] For the synthesis of PCN-222, $ZrCl_4$ (50 mg), H_2TCPP (50 mg) and benzoic acid (2700 mg) in 8 mL of DEF were ultrasonically dissolved in a 20 mL Teflon-lined autoclave. The mixture was heated in an oven at 120 °C for 48 h and then at 130 °C for 24 h. After cooling down to room temperature, purple needle-shaped crystals were harvested by filtration.

Surface modification of OPA on MOFs

Typically, 0.05 g of MOF powder was immersed in 50 mL of 5 mM OPA ethanol solution for 24 h at room temperature during which time the mixture was stirred about once every two hours for five minutes. The solution was then decanted and the remaining solid material was then washed with ethanol three times to make sure excess OPA was removed. The washed material was activated under dynamic vacuum for 24 h at room temperature and at 120 °C for 24 h.

Filtering ability test

A variety of approximately saturated solutions were obtained by adding excess benzene or toluene to 100 mL of water.[27] A stock solution of 200 ppm 1-naphthalenesulfonic acid (NA) was prepared by dissolving 20 mg of solid in 100 mL of deionized water.

Results and discussion

Materials characterisation before and after molecular-level modification

The inclusion of OPA with Zr-based MOFs (abbreviated to OPA-MOFs) was performed using a 5 mM OPA ethanol solution at room temperature by immersing the MOF for 24 h. The phase composition of Zr-based MOFs was observed through the use of

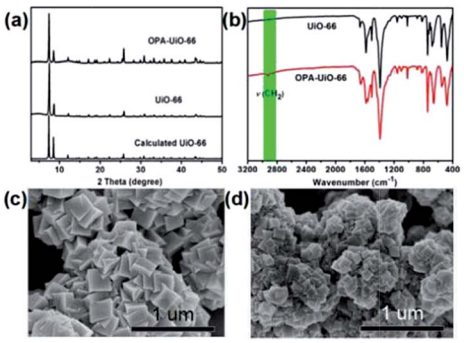

Fig. 1 (a) PXRD patterns and (b) FT-IR spectra of the UiO-66 sample before and after modification with OPA molecules, SEM images of (c) UiO-66 and (d) OPA-UiO-66 samples.

PXRD measurements (Fig. 1a, S1a and b†). The observed PXRD patterns are all in good agreement with the calculated powder patterns, reaffirming the pure MOFs' as-synthesized and post-modified phases. The observed presence of OPA on the MOFs was verified using IR spectroscopy. As shown in Fig. 1b, S1c and d,† the FT-IR spectra of OPA-MOFs revealed the symmetric and asymmetric stretching vibration of the alkyl $-CH_2-$ groups at 2920 and 2850 cm^{-1}. These peaks correlate well with the spectrum of pure OPA (Fig. S2†) and are not present in the IR spectra of the original MOFs.[28,29] The TEM elemental mappings in Fig. 2 also verified the presence of the OPA molecule on the surface of the MOFs. Quantitative analysis of OPA on UiO-66 was conducted *via* ICP-OES. By measuring the phosphorus and zirconium amounts, we calculated the degree of OPA grafting from the ratio between Zr and P. For the OPA-UiO-66, OPA-UiO-66-SO_3H, and OPA-PCN-222 samples, the molar ratio of P:Zr was equal to 0.010, 0.011 and 0.017, respectively. We interpret these results to suggest that successful modification of OPA molecules does not occur throughout the whole crystalline system, but that the grafting does occur within the first few layers of the crystal as observed during elemental mapping.

SEM observations confirmed the intact morphologies of the OPA-MOF crystals. As seen in Fig. 1c and d, there was no significant difference in the UiO-66 crystal morphology besides smaller crystals observed with the OPA-UiO-66 samples. We attribute this decrease in size to the dissolution of the Zr-based

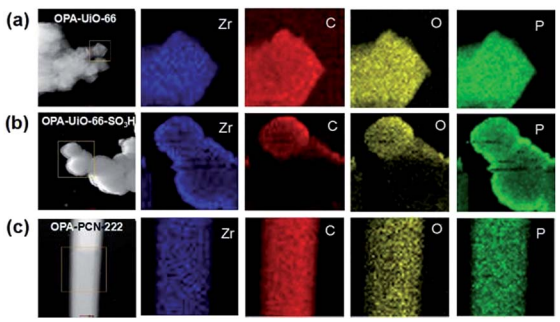

Fig. 2 TEM images and the corresponding elemental mapping of (a) OPA-UiO-66; (b) OPA-UiO-66-SO_3H; and (c) OPA-PCN-222 samples.

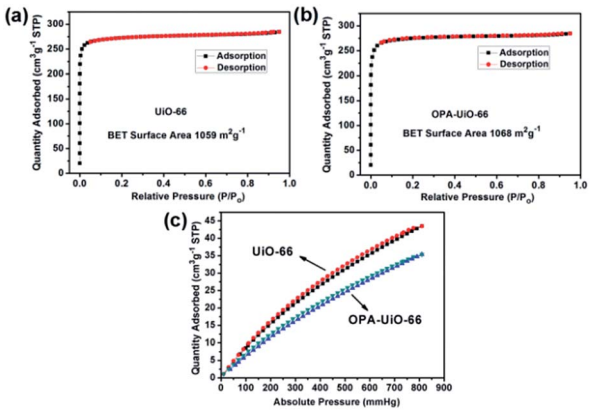

Fig. 3 N_2 sorption isotherms of (a) UiO-66 and (b) OPA-UiO-66 samples, and (c) CO_2 adsorption isotherms of UiO-66 and OPA-UiO-66 samples at 298 K.

MOF in the OPA ethanol solution. This was also observed with the other two Zr-MOFs (Fig. S3a–d†).

External surface modification using OPA

Nitrogen sorption isotherm experiments at 77 K were conducted to examine the possibility of the inclusion of OPA molecules in the pores of the MOFs. The adsorption and desorption isotherms of the three Zr-MOFs before and after adding OPA are shown in Fig. 3a and b and S4a–d.† The calculated BET surface areas of the unmodified and post-modified Zr-MOFs were nearly unchanged at 1059 (1068), 1126 (1148) and 1697 (1618) $m^2\ g^{-1}$ for UiO-66 (OPA-UiO-66), UiO-66-SO_3H (OPA-UiO-66-SO_3H), and PCN-222 (OPA-PCN-222), respectively. Pore size distribution obtained using the DFT method also revealed that little difference was present (Fig. S5a–c†), which demonstrated that this technique, to decorate Zr-MOFs, is useful for modifying the crystal's surface while not significantly affecting its interior free space.[30]

Carbon dioxide isotherms of the UiO-66 and OPA-UiO-66 samples have also been obtained as a comparison study for external OPA modification. The CO_2 sorption capabilities of UiO-66 and OPA-UiO-66 reach 43.4 and 35.3 $cm^3\ g^{-1}$ at 298 K (Fig. 3c) and increased to 70.9 and 61.0 $cm^3\ g^{-1}$ at 273 K and at 810 mmHg (Fig. S6a and b†), respectively. Over 80% of the initial CO_2 capacity was retained after OPA modification, which supports our hypothesis that modification occurred on the crystal's surface.

Superhydrophobicity of OPA-MOFs

Contact angle measurements were performed to examine the hydrophobic properties of OPA-MOF materials. When contact angles are larger than 150°, the material displays superhydrophobic properties, which can find high utility in advanced materials. The contact angle of a water droplet on UiO-66 was estimated to be 19°, which increased to 160° upon OPA modification. This difference of 141° in the contact angle revealed the simplistic nature that OPA modification has when transforming the surface character of the UiO-66 from hydrophilic to

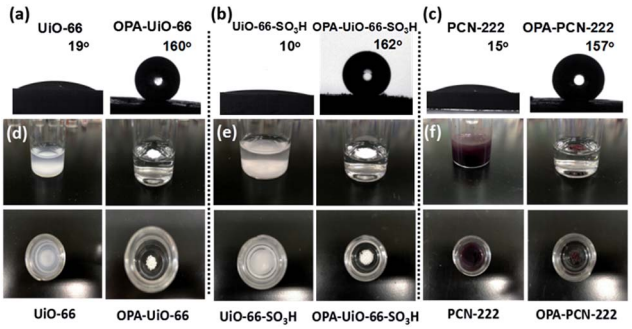

Fig. 4 Contact angle images of (a) UiO-66, (b) UiO-66-SO_3H, and (c) PCN-222 samples before and after OPA modification, and digital photographs of (d) UiO-66, (e) UiO-66-SO_3H, and (f) PCN-222 samples dispersed in water before and after OPA modification.

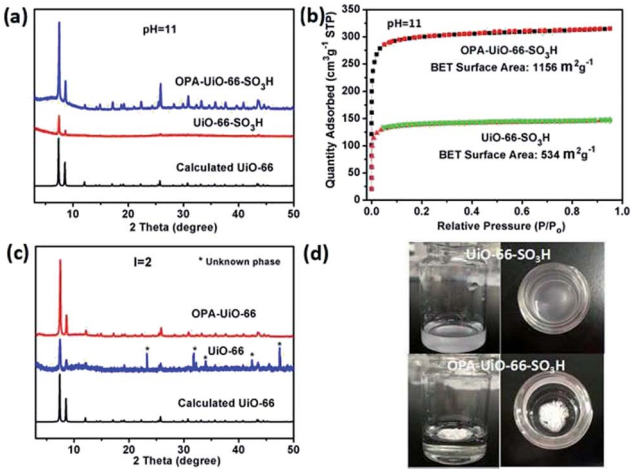

Fig. 5 (a) PXRD patterns and (b) N_2 sorption isotherms of OPA-UiO-66-SO_3H and UiO-66-SO_3H samples after exposure to a basic solution (pH = 11) for 7 and 2 days, respectively, (c) PXRD patterns of OPA-UiO-66 and UiO-66 samples after exposure to a high ionic strength solution, and (d) Digital photographs of UiO-66-SO_3H and OPA-UiO-66-SO_3H samples dispersed in a high ionic strength (I = 2) water solution for 7 days.

superhydrophobic (Fig. 4a). Similarly, OPA-UiO-66-SO_3H and OPA-PCN-222 samples also showed contact angles larger than 150° (Fig. 4b and c). The powder OPA-MOFs can even float on water for at least one month, because the long alkyl chains on the MOF surface, along with their low density, effectively repel water from the MOF powders, making them aggregate on top of the water (Fig. 4d–f). In addition, some recent reports of hydrophobic MOFs are summarized in Table S1,† and compared with other reported hydrophobic MOFs, our OPA modified UiO-66 exhibits a competitive water contact angle value.[9,12,14,19,27,31] In contrast, the OPA-MOFs can be wetted and sink immediately in an oil phase, such as ethyl acetate, toluene, hexane, and heptane (Fig. S7†), suggesting their oleophilicity. All the above results suggest that OPA-MOFs are highly hydrophobic and oleophilic and may show potential in removal of organic pollutants from water, as demonstrated later.

Improved stability of molecular-level modified MOFs

To determine the stability of MOFs after external superhydrophobic modification, OPA-UiO-66-SO_3H and OPA-PCN-222 were chosen and exposed to basic solutions since these Zr-based MOFs are known to be stable in acidic environments (Fig. S8†).[32,33] PXRD patterns of these OPA-MOFs after exposure to basic (pH = 11) conditions for 7 days remained unchanged as can be observed in Fig. 5a and S9,† revealing the integrity of the OPA-MOFs framework structure under basic conditions. In addition, the surface areas of these OPA modified MOFs were retained after exposure to basic conditions (pH = 11). The BET surface areas of OPA-UiO-66-SO_3H and OPA-PCN-222 were 1156 and 1713 $m^2\ g^{-1}$, respectively (shown in Fig. 5b and S10†). In stark contrast, the diffraction peaks of UiO-66-SO_3H become very weak or disappear after exposure to the basic solution (pH = 11) for 2 days, and the BET surface area of UiO-66-SO_3H sample was reduced by 53.8% from 1156 to 534 $m^2\ g^{-1}$. The unmodified PCN-222 sample was destroyed in the basic solution (pH = 11) that resulted in a transparent purple coloured solution as shown in Fig. S11.† We can conclude that OPA external modification of the MOFs resulted in improved tolerability to basic solution conditions.

To test the stability of these materials in a high ionic strength solution, the samples were exposed to a solution of 0.5 M NaCl and 0.5 M Na_2SO_4. Visually and crystallographically OPA-UiO-66 appeared unchanged in contrast with UiO-66 that showed new peaks in the PXRD pattern (Fig. 5c) after exposure to the high ionic strength (I = 2) solution for 7 days. These new peaks may suggest that the metal and ligand (Zr and terephthalate) in UiO-66 are being exchanged with the ions in solution. Surprisingly, the UiO-66-SO_3H sample decomposed in the high ionic strength (I = 2) solution after similar exposure as shown in Fig. 5d. OPA-UiO-SO_3H powders remained stable after the same exposure as shown by their PXRD pattern in Fig. S12.† This trend, whereby OPA-MOFs exhibited better stability than the unmodified MOFs under various aqueous conditions should be resourceful in removing contaminants from industrial waste or oil spills.

Effect of molecular-level external modification on molecular filtering of MOF windows

To examine the contaminant filtering abilities of OPA-MOFs, benzene, toluene, and naphthalenesulfonic acid (NA) saturated solutions in water were prepared. To determine contaminant removal, a series of UV/Vis absorption experiments were carried out by adding 10 mg of the powders into 10 mL of the saturated solutions. After dispersing the OPA-UiO-66-SO_3H sample in the benzene and toluene solution for 1, 6, 12, and 24 h, the UV/Vis spectra revealed that approximately 95.4% of benzene and 98.9% of toluene were removed from solution (Fig. 6a and c). In sharp contrast, the UV/Vis spectra of the UiO-66-SO_3H sample in the same solution for 1, 6, 12, and 24 h showed that the decreasing trend of absorbance of unmodified MOFs toward toluene and benzene was obviously slower than that of the OPA-UiO-66-SO_3H sample, particularly within 6 h

(Fig. 6b and d). Different absorption behaviors of OPA-UiO-66-SO_3H and UiO-66-SO_3H were observed using a larger molecule. As shown in Fig. 6e, after soaking OPA-UiO-66-SO_3H in the NA solution, no obvious changes were observed in the absorbance intensity, indicating that no NA molecules were absorbed within the OPA modified MOF, likely due to a decrease in the window size after OPA external modification. For comparison, UiO-66-SO_3H was shown to decrease the NA concentration significantly over a 24 hour period (Fig. 6f). These results revealed that OPA-MOFs can accelerate the removal rate of small-sized organic pollutants from water. Importantly, the molecular-level external modification can greatly improve the molecular filtering properties of porous MOFs owing to the change in window size, which may allow OPA-MOFs to exhibit size selective separations.

Organic solvent absorption

The absorption capacity towards organic solvents was evaluated in a similar manner reported by Li *et al.*[34] In a typical absorption measurement, the OPA modified sample was immersed in toluene at room temperature and left to rest for 5 min for saturated absorption, then centrifuged to collect the solid, and finally weighed. The absorbency, defined as $Q = (W_{\text{saturated absorption}} - W_{\text{initial}})/W_{\text{initial}} \times 100\%$, is employed to measure how much organic phase was caught by the materials. As shown in Fig. 7, UiO-66 and OPA-UiO-66 both show high absorption capacities. These high uptake values can be attributed to the high surface area and the hydrophobic interior of the MOF materials even after OPA modification. The PXRD pattern and FT-IR spectra confirm that the structural properties of the OPA-UiO-66 sample are fully retained after absorbing these organic solvents (Fig. S13†), highlighting the intact nature of the OPA-MOFs.

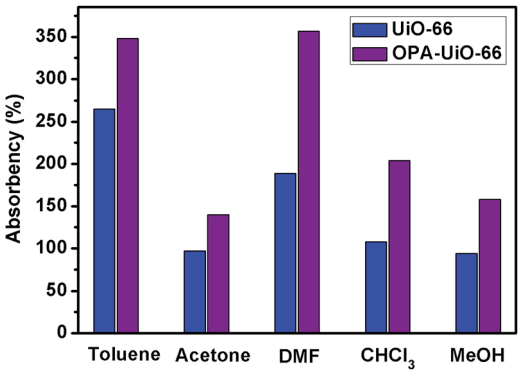

Fig. 7 Absorption of organic solvents with UiO-66 before and after OPA modification.

Oil/water separation

With these promising results, practical oil/water separation experiments were also carried out since the OPA-MOF surfaces display superhydrophobicity and oleophilicity.[35] Fig. 8a demonstrates that the OPA-UiO-66 sample is highly hydrophobic in water and oleophilic in chloroform. The separation device was homemade and fabricated according to a previous report.[27] Similarly, a piece of gauze was placed on the bottom of a syringe, on which was placed the MOF sample, which was then readied by flowing nitrogen gas through the syringe to fasten the MOF (plug) onto the gauze. After generating the filter device, a chloroform/water separation was tested. Fig. 8b–d show the equipment images of the separation process and the mixture of chloroform and water before and after separation through the OPA-MOF samples. When a mixture of water (dyed by methylene blue) and chloroform was gravity fed into the syringe tube, chloroform freely passed through the OPA-MOF sample and fell

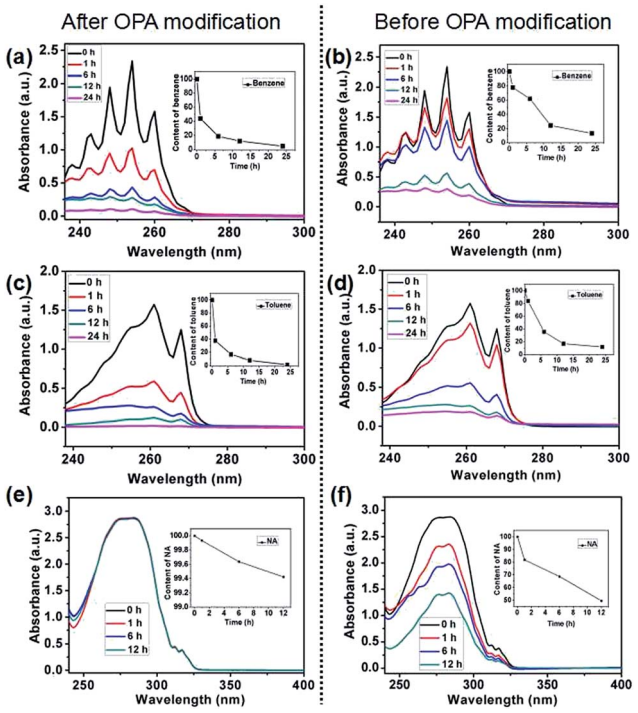

Fig. 6 UV-Vis spectra of organic molecules in water with MOFs before and after OPA modification, (a) benzene, OPA-UiO-66-SO_3H, (b) benzene, UiO-66-SO_3H, (c) toluene, OPA-UiO-66-SO_3H, (d) toluene, UiO-66-SO_3H, (e) NA, OPA-UiO-66-SO_3H and (f) NA, UiO-66-SO_3H. The inset is the corresponding content of organic molecules as a function of time.

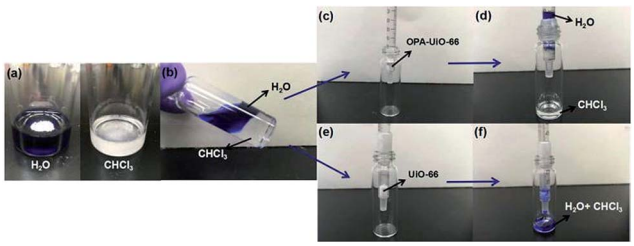

Fig. 8 Digital photographs of (a) OPA-UiO-66 samples dispersed in water and chloroform, (b–d) the OPA-MOF based water/oil separation process of water and chloroform and (e–f) the unmodified MOF based separation process. The water was dyed with methylene blue for clear observation.

into the vial beneath it, but water could not penetrate the hydrophobic OPA modified sample. The same test showed both phases passing through the unmodified MOF (Fig. 8e and f). These results suggest that the hydrophobic OPA-MOF exhibits an efficient organic/water separation ability, which would offer a considerable application prospect for oil/water separation.

Conclusions

In summary, we have reported a facile method to modify the external surface of MOFs with superhydrophobicity through incorporation of *n*-octadecylphosphonic acid. The integration of OPA with long alkyl chains not only retains the inherent porosity and surface area of the pristine MOF, but also provides a high level of resistance to acidic/basic aqueous solutions as shown experimentally in their PXRD patterns and measured BET surface area data. Furthermore, the present OPA-MOFs exhibit molecular filtering effects due to the external molecular-level modification as well as their large potential in fast removal of organic pollutants from water. Such a facile and straightforward strategy would open a new avenue to protect porous MOF materials under various environments and promote MOF materials capable of practical applications. This superhydrophobic modification strategy may be extended to other metal-based MOFs like those composed of Ti, Zr, Zn, and Al, owing to the strong coordination bonding between OPA and these metals.

Conflicts of interest

There are no conflicts to declare.

Acknowledgements

We would like to thank financial support from the Natural Science Foundation of China (21403155), the Tianjin Natural Science Foundation (15JCYBJC17600) and the China Scholarship Council (201608120045). The authors also acknowledge the National Science Foundation (NSF), USA (grant number DMR-1352065) and the University of South Florida (USF) for partial support of this work.

Notes and references

1 H. C. Zhou, J. R. Long and O. M. Yaghi, *Chem. Rev.*, 2012, **112**, 673.
2 S. M. Cohen, *Chem. Rev.*, 2012, **112**, 970.
3 C. Serre, *Angew. Chem., Int. Ed.*, 2012, **51**, 6048.
4 R. Banerjee, H. Furukawa, D. Britt, C. Knobler, M. OKeeffe and O. M. Yaghi, *J. Am. Chem. Soc.*, 2009, **131**, 3875.
5 J. J. Low, A. I. Benin, P. Jakubczak, J. F. Abrahamian, S. A. Faheem and R. R. Willis, *J. Am. Chem. Soc.*, 2009, **131**, 15834.
6 V. Colombo, S. Galli, H. J. Choi, G. D. Han, A. Maspero, G. Palmisano, N. Masciocchic and J. R. Long, *Chem. Sci.*, 2011, **2**, 1311.
7 T. Wu, L. Shen, M. Luebbers, C. Hu, Q. Chen, Z. Ni and R. I. Masel, *Chem. Commun.*, 2010, **46**, 6120.
8 H. Jasuja, Y. G. Huang and K. S. Walton, *Langmuir*, 2012, **28**, 16874.
9 C. Liu, Q. Liu and A. Huang, *Chem. Commun.*, 2016, **52**, 3400.
10 C. Yang, U. Kaipa, Q. Z. Mather, X. Wang, V. Nesterov, A. F. Venero and M. A. Omary, *J. Am. Chem. Soc.*, 2011, **133**, 18094.
11 Q. Sun, H. M. He, W. Y. Gao, B. Aguila, L. Wojtas, Z. F. Dai, J. X. Li, Y. S. Chen, F. S. Xiao and S. Q. Ma, *Nat. Commun.*, 2016, **7**, 13300.
12 S. Roy, V. M. Suresh and T. K. Maji, *Chem. Sci.*, 2016, **7**, 2251.
13 K. P. Rao, M. Higuchi, K. Sumida, S. Furukawa, J. Duan and S. Kitagawa, *Angew. Chem., Int. Ed.*, 2014, **126**, 8364.
14 S. Mukherjee, A. M. Kansara, D. Saha, R. Gonnade, D. Mullangi, B. Manna, A. V. Desai, S. H. Thorat, P. S. Singh, A. Mukherjee and S. K. Ghosh, *Chem.–Eur. J.*, 2016, **22**, 10937.
15 A. Carne-Sanchez, K. C. Stylianou, C. Carbonell, M. Naderi, I. Imaz and D. Maspoch, *Adv. Mater.*, 2015, **27**, 869.
16 W. Zhang, Y. L. Hu, J. Ge, H. L. Jiang and S. H. Yu, *J. Am. Chem. Soc.*, 2014, **136**, 16978.
17 C. A. Fernandez, S. K. Nune, H. V. Annapureddy, L. X. Dang, B. P. McGrail, F. Zheng, E. Polikarpov, D. L. King, C. Freeman and K. P. Brooks, *Dalton Trans.*, 2015, **44**, 13490.
18 G. Huang, Q. H. Yang, Q. Xu, S. H. Yu and H. L. Jiang, *Angew. Chem., Int. Ed.*, 2016, **55**, 7379.
19 X. Qian, F. Sun, J. Sun, H. Wu, F. Xiao, X. Wu and G. Zhu, *Nanoscale*, 2017, **9**, 2003.
20 Z. Q. Wang and S. M. Cohen, *Chem. Soc. Rev.*, 2009, **38**, 1315.
21 R. Boissezon, J. Muller, V. Beaugeard, S. Monge and J.-J. Robin, *RSC Adv.*, 2014, **4**, 35690.
22 G. Guerrero, P. H. Mutin and A. Vioux, *Chem. Mater.*, 2001, **13**, 4367.
23 T. Schulmeyer, S. A. Paniagua, P. A. Vaeneman, S. C. Jones, P. J. Hotchkiss, A. Mudalige, J. E. Pemberton, S. R. Marder and N. R. Armstrong, *J. Mater. Chem.*, 2007, **17**, 4563.
24 J. H. Cavka, S. Jakobsen, U. Olsbye, N. Guillou, C. Lamberti, S. Bordiga and K. P. Lillerud, *J. Am. Chem. Soc.*, 2008, **130**, 13850.
25 M. Lin Foo, S. Horike, T. Fukushima, Y. Hijikata, Y. Kubota, M. Takata and S. Kitagawa, *Dalton Trans.*, 2012, **41**, 13791.
26 H. Q. Xu, J. Hu, D. Wang, Z. Li, Q. Zhang, Y. Luo, S. H. Yu and H. L. Jiang, *J. Am. Chem. Soc.*, 2015, **137**, 13440.
27 M. Zhang, X. Xin, Z. Xiao, R. Wang, L. Zhang and D. Sun, *J. Mater. Chem. A*, 2017, **5**, 1168.
28 I. A. Lázaro, S. Haddad, S. Sacca, C. Orellana-Tavra, D. Fairen-Jimenez and R. S. Forgan, *Chem*, 2017, **2**, 561.
29 X. Guo, D. Liu, T. Han, H. Huang, Q. Yang and C. Zhong, *AIChE J.*, 2017, **63**, 1303.
30 J. Chun, S. Kang, N. Park, E. J. Park, X. Jin, K. Kim, H. O. Seo, S. M. Lee, H. J. Kim, W. H. Kwon, Y. Park, J. M. Kim, Y. D. Kim and S. U. Son, *J. Am. Chem. Soc.*, 2014, **136**, 6786.
31 H. N. Rubin and M. M. Reynolds, *Inorg. Chem.*, 2017, **56**, 5266.

32 J. Juan-Alcaniz, R. Gielisse, A. B. Lago, E. V. Ramos-Fernandez, P. Serra-Crespo, T. Devic, N. Guillou, C. Serre, F. Kapteijin and J. Gascon, *Catal. Sci. Technol.*, 2013, **3**, 2311.
33 D. Feng, Z. Y. Gu, J. R. Li, H. L. Jiang, Z. Wei and H. C. Zhou, *Angew. Chem.*, 2012, **124**, 10453.
34 A. Li, H. X. Sun, D. Z. Tan, W. J. Fan, S. H. Wen, X. J. Qing, G. X. Li, S. Y. Li and W. Q. Deng, *Energy Environ. Sci.*, 2011, **4**, 2062.
35 P. Z. Li, X. J. Wang, S. Y. Tan, C. Y. Ang, H. Chen, J. Liu, R. Zou and Y. Zhao, *Angew. Chem., Int. Ed.*, 2015, **54**, 12748.